International Journal of Solids and Structures 47 (2010) 2294–2299

Contents lists available at ScienceDirect

International Journal of Solids and Structures

journal homepage: www.elsevier.com/locate/ijsolstr

# Study of a drawing-quality sheet steel. II: Forming-limit curves by experiments and micromechanical simulations

G. Charca Ramos [a], M. Stout [a,*], R.E. Bolmaro [a,b], J.W. Signorelli [a,b], M. Serenelli [a], M.A. Bertinetti [a,b], P. Turner [a,b]

[a] Instituto de Física Rosario (IFIR), CONICET – UNR, 27 de febrero 210 bis (2000), Rosario, Argentina
[b] Facultad de Ciencias Exactas, Ingeniería y Agrimensura, Universidad Nacional de Rosario, Pellegrini 250 (2000), Rosario, Argentina

ARTICLE INFO

*Article history:*
Received 9 October 2009
Received in revised form 19 February 2010
Available online 28 April 2010

*Keywords:*
Forming-limit curve
Lankford coefficient
Formability
Yield
Flow

ABSTRACT

In Part I of the current paper, we showed the results of uniaxial-tension tests, through-thickness and plane-strain compression experiments, quantitative texture – orientation distribution function – evaluations and Lankford coefficient measurements. These data were used for calibration and verification of a visco-plastic self-consistent (VPSC) polycrystal-plasticity simulation code for predicting a steel sheet's ability to be stretched and deep drawn. Lankford coefficients are one, although incomplete, measure of a steel's drawing quality. In order to obtain a deeper insight and better verification of the simulation code, we measured the forming-limit curve, FLC, for the same steel sheet. To make these measurements we stretched circle-gridded sheets of material with a punch and die. Samples had both a flat-sided and hour-glass geometry and ranged from 20 to 80 mm in width. The 80 mm wide sample completely filled the die. With this range of sample sizes, we spanned all of the stress states applicable to a FLC, from uniaxial to biaxial tension. Our FLC curve had the classic "V" shape typical of drawing-quality steel, with a minimum safe forming strain of about 0.35 in plane-strain deformation and a safe forming strain of nearly 0.45 in balanced biaxial stretching. To model the FLC behavior, we used the same VPSC model and calibration employed in Part I. In order to obtain a necking instability in the calculation, a Marciniak defect was implemented into the VPSC model. The severity of the defect was adjusted to match the measured instability strain, 0.35, in plane-strain deformation. Both hardening laws fit in Part I were used to calculate the FLC. In the positive biaxial quadrant of the FLC, the limit strains predicted by the power law closely follow the measured uniform deformations, while the saturation law appears to over predict the limit strains. In uniaxial-tension, it was the opposite. The power-law hardening predictions seemed excessive. However, if we consider the FLC curve to be a band of finite width, both hardening laws and the VPSC formulation capture the essence of the FLC data.



## 1. Introduction

The forming-limit curve or FLC is one of the best tools available to metallurgical engineers to assess a particular steel sheet's ability to be drawn or stretched. The FLC is either a curve or band of finite width that is plotted in the in-plane strain space of a material sheet. Extending between uniaxial and balanced biaxial-tension stress states, the FLC separates the region of uniform sheet deformation from the region of slightly greater deformation, where the sheet will likely develop a local deformation instability or neck. The concept of the FLC is most applicable to the stretching process, in which the boundaries of the sheet being formed are fixed.

Simulations of metal forming, in particular simulations of forming-limit curves, have advanced dramatically in recent years, with the incorporation of various anisotropic yield functions and crystal-plasticity models in simulation codes. These simulations are based on describing a material's yield function and subsequent flow surfaces and then incorporating an instability analysis – for example a Marciniak defect – to initiate localized plastic flow. The investigations by Knockaert et al. (2002), Kuroda and Kuwabara (2002), Barlat et al. (2003), Wu et al. (2003), McGinty and McDowell (2004), Abedrabbo et al. (2006), Campos et al. (2006), Aretz (2007), Ganjiani and Assempour (2007), Yoshida et al. (2007) and Signorelli et al. (2009) among others, are some of the most notable recent examples of this type of theoretical simulation of metal formability.

While the simulation techniques applicable to metal forming have made significant advances, researchers are still limited by the lack of a complete data set for any particular material. FLCs and Lankford coefficients are now available for many drawing-quality steels, but these data are rarely accompanied by quantita-

* Corresponding author. Tel./fax: +54 341 480 8545.
*E-mail address:* stout_michael@yahoo.com (M. Stout).

0020-7683/$ - see front matter © 2010 Elsevier Ltd. All rights reserved.
doi:10.1016/j.ijsolstr.2010.04.022

tive texture measurements that can be input into the crystal-plasticity based theories, a requirement for FLC prediction. Currently, most researchers conducting simulations must make assumptions with respect to the material's texture.

The objective of our research was to implement the comprehensive data set discussed in Part I for our particular steel sheet into a visco-plastic self-consistent, VPSC, polycrystalline model and then to use this model to predict the steel's FLC. The model's predictions will be validated by comparison to the measured FLC.

Since Keeler and Backhofen (1964) introduced the concept of the FLC, this diagram has been a useful tool for predicting sheet-metal stretchability, for a wide variety of conditions and strain states. Although this tool has been refined over the years, the basic concept of the FLC and the methods for measuring it have remained unchanged. A sample of the sheet material is marked with a grid pattern to track deformation and mounted in a circular die such that the edges of the sheet are fixed. A punch is then pushed through the die deforming the material. Generally, this process continues until the sheet develops a plastic-flow instability, which would eventually lead to fracture. Investigators assess the strains associated with uniform deformation and the plastic-flow instability, necking, by measuring the grid pattern, usually a circular pattern, before and after deformation. Hecker (1975) has given a detailed description of punch and die designs as well as the specific techniques for measuring the FLC.

Different sheet-sample widths and geometries and various lubrications between the punch and die can produce strain states between uniaxial and balanced biaxial tension, including plane-strain deformation, in the FLC experiment. A wide, well-lubricated sheet completely clamped around the edge gives a nearly biaxial strain state while a narrow sheet also well lubricated tends towards uniaxial-tension. For incomplete samples, those not completely gripped around the circumference, either a flat-sided (Ravi Kumar, 2002; Narayanasamy and Sathiya Narayanan, 2006; Kim et al., 2003; Aghaie-Khafri et al., 2002; Gupta and Ravi Kumar, 2006; Janssens et al., 2001; Raghavan, 1995) or hourglass-shaped geometry (Raghavan, 1995; Holmberg et al., 2004; Hiroi and Nishimura, 1997) has been used with seemingly equal success.

Investigators have also varied punch geometries in performing FLC measurements. A hemispherical-shaped punch is the simplest design to use, but this geometry produces significant strain gradients. To avoid these gradients, early on, Azrin and Backofen (1970) and Marciniak and Kuczynski (1967) developed techniques for obtaining uniform stretching deformation in FLC experiments. Controversy later developed when Ghosh and Hecker (1974) reported that FLC results from their pure-stretching measurements did not match those that they had obtained using the hemispherical-punch geometry. Raghavan (1995) expanded on the work of Gosh and Hecker with a series of hemispherical and pure-stretching experiments on two steel sheets: a low-carbon, drawing-quality steel and an interstitial-free steel. Following the technique of Hecker (1975), Raghavan produced a forming-limit curve with a hemispherical punch and compared these results to pure-stretching experiments he performed using the (Marciniak and Kuczynski, 1967) (M–K) technique of applying the load through a washer with a blunt-nose punch. Raghavan's two forming-limit curves for both steels deviated by at most 5% strain for the different techniques. Raghavan noted that, to obtain a state of pure stretching deformation, Ghosh and Hecker had thinned a region of their sheet by about 50%, and he attributed their results to this thickness difference.

## 2. Micromechanical simulations

For a complete description of the VPSC model we refer the reader to Part I of this paper and to Lebensohn and Tomé (1993).

The original Marciniak and Kuczynski (1967) approach is characterized by the existence of a material imperfection such as a groove or a narrow band across the width of the sheet. In the modified model, proposed by Hutchinson and Neale (1978), the orientation of the band is determined by an angle $\Psi$ with respect to the $x_2$ reference direction, see Fig. 1. Tensor components are taken with respect to the Cartesian $x_i$ coordinate system. Quantities inside the band are denoted by subscript $b$.

The thickness along the minimum section in the band is denoted by $h_b(t)$, with an initial value $h_b(0)$. The imperfection factor is given by the initial thickness ratio inside and outside the band:

$$f = \frac{h_b(0)}{h(0)} \tag{1}$$

with $h(0)$ being the sheet's initial thickness outside the groove.

Equilibrium and compatibility conditions have to be fulfilled at the interface with the band. Following the formulation developed by Wu et al. (1997), the compatibility condition at the band interface is given in terms of the differences between the velocity gradients $(L^b, L)$ inside and outside the band respectively:

$$L^b_{ij} = L_{ij} + \dot{c}_i n_j \tag{2a}$$

Eq. (2a) is decomposed into the symmetric $D$ and screw-symmetric $W$ parts:

$$D^b_{ij} = D_{ij} + \frac{1}{2}(\dot{c}_i n_j + n_i \dot{c}_j)$$
$$W^b_{ij} = W_{ij} + \frac{1}{2}(\dot{c}_i n_j - n_i \dot{c}_j) \tag{2b-c}$$

Here, $n_j$ are the components of the unit normal to the band, and $\dot{c}_i$ are parameters to be determined. The equilibrium conditions required at the band interface are given by:

$$n_i \sigma^b_{ij} h_b = n_i \sigma_{ij} h \tag{3}$$

where, $\sigma$ denotes Cauchy stress. The boundary condition $\sigma_{33} = 0$ is applied as follows ($\delta_{ij}$ is the Kronecker symbol):

$$\sigma_{ij} = s_{ij} - s_{33}\delta_{ij} \tag{4}$$

From Eqs. (2)–(4) and the macroscopic polycrystal second relation, a set of equations to solve $\dot{c}_i$ were obtained through the incremental form of Eq. (3), using Eq. (2b) to eliminate the strain increments in the band. At any increment of strain along the prescribed strain path, the nonlinear system of two equations is solved. The minimum strain state $\varepsilon^*_{11}$, $\varepsilon^*_{22}$[1] outside the band for various initial inclinations of the groove are defined as the forming-limit strains. In the present work, the failure condition is reached when $D^b_{11} > 20D_{11}$. The details for this implementation can be found in Signorelli et al. (2009).

## 3. Experimental procedure

While we are only concerned with experiments to characterize the FLC in this paper, Part II, the reader should note that we are using the identical material described in Part I. All of the material characterizations presented there – composition, texture and mechanical properties – are still applicable and will not be repeated here.

Following the work of Hecker (1975), we designed the punch and die shown in Fig. 2, for performing the FLC measurements. The die accepts disks of sheet material that are 80 mm in diameter, fixing them in place with a draw bead equivalent to that used by other researchers Hecker (1975), Ravi Kumar (2002). A recess

[1] For simplicity, in all figures, the limit strains are denoted by $\varepsilon_1$ and $\varepsilon_2$ instead of $\varepsilon^*_{11}$ and $\varepsilon^*_{22}$.

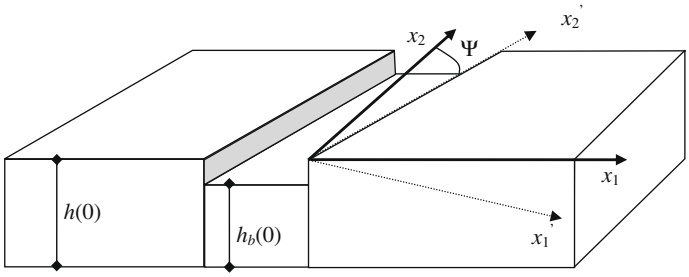


**Fig. 1.** Initial defect approach.

45 mm in diameter accommodates the extension of the sheet and provides lateral relief for the 40 mm diameter hemispherical punch. A 1.5 mm edge radius accommodates the entry of the sheet into the die. As discussed in the Part I paper, the sheets tested in this investigation were 0.6 mm thick. The die cap, which centers the punch through a slip fit, is held in place by eight bolts arranged in a symmetric pattern.

We designed the FLC samples with the objective of obtaining distinct deformation paths in strain space, from uniaxial to balanced-biaxial tension, including plane-strain deformation. The tests employed three unique geometries: a complete circular disk 80 mm in diameter, an hourglass geometry with widths of 20, 30, 40, 50 and 60 mm and a flat-sided sample, 20, 30 and 40 mm in width. These various geometries are illustrated in Fig. 3. All of the specimens were fabricated by laser cutting and their edges polished with metallographic papers before testing. Besides geometry, the lubrication used between the punch and sample affects the strain path the sample will follow. We employed three forms of lubrication. When testing with the complete disk to obtain balanced-biaxial deformation, a 40 mm diameter disk of elastomeric polymer about 8 mm thick was used. This disk flows like a viscous oil and it provides as close to a frictionless condition as is possible. For the partial disks of both geometries, two lubricants were used, either separately or together, the Molykote® spray lubricant and a sheet of cast Teflon. In all experiments with the hourglass or flat-sided sample geometry, the side of the sample that was going to be in contact with the punch was sprayed with the Molykote® aerosol lubricant. For some cases, a sheet of cast Teflon was also inserted between the sample and punch. The punch was never painted with the Molykote® lubricant. Rather, we always used it in a bare, polished condition. A circle grid, applied to the opposite side of the sheet from the punch, provided a method of measuring the local deformations attained through the stretching process. We applied the grid of 2.7 mm diameter circles using equipment manufactured by the Lectroetch Company of Sheffield, Ohio. Prior to deformation, a single digital photograph of the gridded sample and a ruler recorded the exact dimensions of each circle in the grid. After the experiment, through visual inspection, we identified which circles had experienced the largest amounts of uniform deformation and which circles suffered localized necking. Each of these particular circles was photographed again with a length scale in the photograph. Care was taken to place the ruler at the same distance from the camera lens as the circles being photographed. Using a computer-aided design program, the photographs of the individual circles were measured to assess the local strain in each. In the case of the deformed circles, we measured the major and minor axes of deformation, which might not lie parallel to the specimen's axes of symmetry. A circle-gridded specimen prior to deformation and the same specimen after testing are shown in Fig. 4. In Fig. 4, the reader can note the identified circles and observe a local neck which has formed in circles 2, 3 and 4.

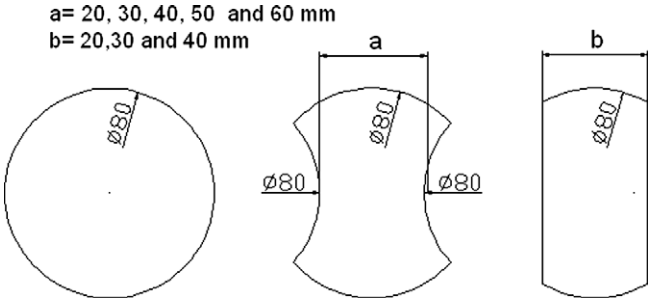


**Fig. 3.** The geometries of the specimens used to establish the FLC.

We tested all specimens using a fixed punch velocity of 0.5 mm/min, irrespective of the sample geometry, lubrication or desired strain path. These tests were conducted in an Instron model

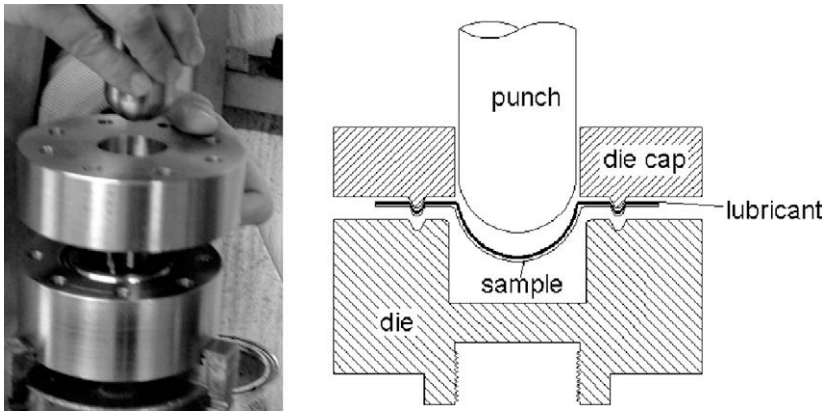


**Fig. 2.** The punch, die and die cap used for measuring the FLC.

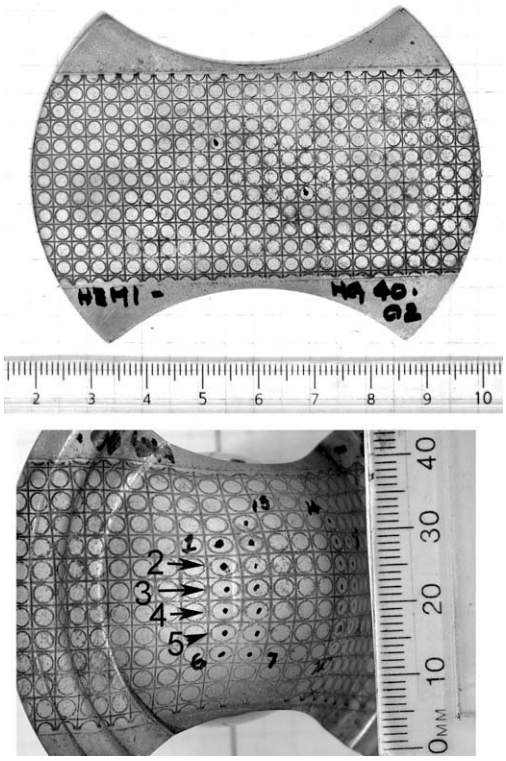


**Fig. 4.** A photograph of a gridded FLC specimen prior to testing, and the same specimen after the test. Circles 2–4 contain a region of localized necking, appearing as a light vertical line.

1362 universal tester with a load capacity of 100 kN, which recorded and displayed the load and crosshead – punch – displacement. During the test, as soon as we visually noted a drop in the load, the experiment was halted. This allowed us to deform the specimens to the point of necking without developing a fracture. This manual procedure resulted in a load drop of about 2% when halting the test. The biaxial specimens were an exception. In this case, the elastomer plug, serving as a fluid, released a sufficient amount of energy through the local necking process to fracture the specimen.

In all cases, except for the 20 mm wide, hour-glass sample, the neck originated and was contained on the sample surface, leading us to believe that edge effects from the laser cutting process did not influence our results. Necking of the 20 mm wide hour-glass sample, which followed a nearly uniaxial-tension strain path, did initiate at the specimen edge, and in this unique case edge effects might have been important. None of the samples, either flat sided or hourglass cracked at the clamping bead, although when the die bolt pressure was insufficient particular flat-sided specimens drew across the clamping bead.

## 4. Results

We found that the measured FLC was consistent with literature data for a drawing-quality steel, and that simulations of the FLC accurately matched our experimental data.

### 4.1. Experimental forming-limit curve

Fig. 5 shows the data obtained through the punch and die stretching experiments. In this figure we are plotting the maximum principal strain measured in individual circles along the *y*-axis and the minimum principal strain along the *x*-axis. The different strain paths and the dispersion in points resulted from different sample geometries and lubrications. In Fig. 5, the solid symbols indicate uniform deformation, and they define a safe zone for metal forming. The open symbols are from measurements of circles that experienced local necking, specifying an insecure zone for metal forming. We have fitted a curve between these two zones and thus obtained the FLC for this particular steel. The maximum deformations that can be expected in forming this steel, as defined by the FLC, occur in the states of uniaxial and balanced biaxial tension, 55% and 45% maximum principal strain respectively. The minimum forming deformation is 35%, occurring in plane-strain

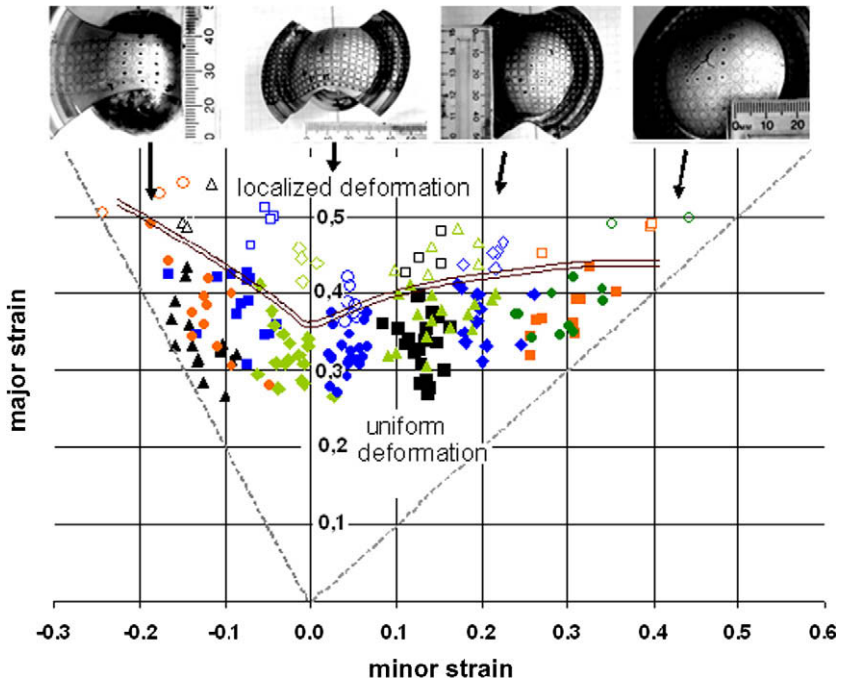


**Fig. 5.** The data and an approximate forming-limit curve for the steel investigated in this study.

deformation. Because failures during production typically occur in the regions of sheet experiencing plane-strain deformation and this is the minimum amount of deformation the sheet can support, it is important to obtain this value accurately and definitively. While the illustrative specimens shown in Fig. 5 all have an hour-glass geometry, data from a 40 mm wide, flat-sided sample are included in the plot. The 20 and 30 mm wide flat-sided specimens experienced a diffuse tensile neck between the die entrance and punch radius, rather than localized necking over the punch. Because such necking is inconsistent with the FLC, data from these samples is not presented in Fig. 5.

As can be seen from the sample photographs in Fig. 5, samples with a complete circular geometry approached balanced-biaxial deformation. The better the lubrication the closer the samples are to a pure biaxial state. Samples with an hourglass shape and an intermediate width – 40 and 50 mm – gave nearly plane-strain deformation, while the narrowest samples – 20 and 30 mm – tended towards a uniaxial-tension deformation state. The 40 mm wide flat-sided sample also tended towards uniaxial tension.

The separation between safe and insecure deformation data is generally very narrow. The exception is in pure biaxial deformation, where the elastomeric disk was used for lubrication. Here the separation between measured uniform and localized – fracture – deformations is between 5% and 10%. We believe this is a result of energy being stored in the disk during deformation. At the point of necking, the disk releases energy into the sample, driving the local neck to greater deformations and fracture.

We constructed the FLC with some points that were apparently deforming uniformly lying above the curve and only three points that might have necked below the curve. Thus, the FLC is conservative, and if a strain state lies below the curve, we can be assured that the deformation is secure, without the possibility of necking.

### 4.2. Simulated forming-limit curve

The simulated FLCs are shown in Fig. 6 for both the power-law hardening and saturation hardening models. Together with the predictions, we have plotted the experimental data from Fig. 5.

In order to utilize the Marciniak approach for numerically initiating a necking instability, it was necessary to specify the imperfection factor, $f_0$, or the specimen thickness within the Marciniak defect to that of the sheet, see Eq. (1). We adjusted $f_0$ such that the predicted FLCs matched the experimental results in plane strain, at a critical-strain value – separating uniform and localized deformation – of 0.35. For the saturation and power-law hardening laws these values of $f_0$ were 0.999 and 0.997 respectively.

Examining the FLC predictions in the biaxial quadrant of stress space, we observed that the FLC predicted by the power-law hardening accurately separates the regions of safe, uniform, and insecure, localized, deformation. The predictions made with the saturation hardening law are not as accurate or conservative. This FLC lies above that from the power law, by about 5%, clearly in the region of localized flow.

On the tensile side of plane strain the situation is reversed. In this case, the saturation law appears to be the more accurate of the two, with the power law predicting excessive uniform deformation, 0.67 in pure uniaxial-tension.

If we were to think of the FLC as a band rather than a single line, the curves from the two hardening laws might be taken as forming the borders of this band.

## 5. Discussion and conclusions

Just as the anisotropic flow behavior of this steel appears to follow conventional wisdom, Part I, its formability behavior also matches the previous results of Ravi Kumar (2002), Gupta and Ravi Kumar (2006), Janssens et al. (2001) and Raghavan (1995). Literature data exhibit a forming limit of about 0.35 in plane strain, as we measured, and they increase to about 0.45 in biaxial tension for standard-grade, drawing-quality steels. These numbers are elevated when higher-quality, interstitial-free and extra deep-drawing steels are considered. Investigators who conducted these previous studies typically drew their FLC curves higher in uniaxial-tension than we did. This, however, appears to be a matter of choice rather than necessity as both the literature studies and ours lack sufficient data to define this point unequivocally. The work of Janssens et al. (2001) is perhaps the most precise, using a statistical approach to specify FLC behaviors. These authors report FLC values in uniaxial-tension – for a slightly lower grade of steel as reflected by the Lankford coefficients – equivalent to ours.

The greatest discrepancies in our FLC predictions between the two hardening laws are in the stress states of uniaxial and balanced biaxial tension. Unfortunately, these are the two stress

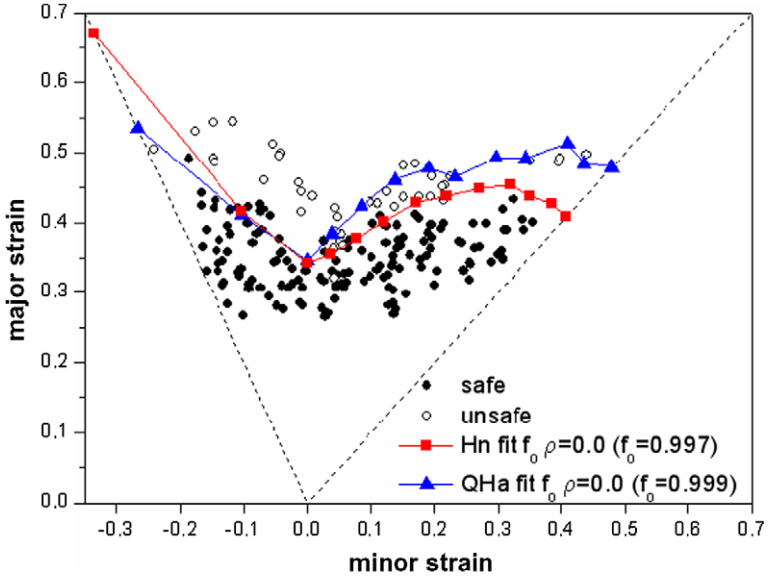


**Fig. 6.** The experimental FLC data from Fig. 5 plotted with the results of the VPSC simulations for both the power-law and saturation hardening models.

states for which it is most difficult to obtain accurate experimental data.

In biaxial tension, we observe a gap of about 5% between uniform and localized strains. This gap resulted from energy in the elastomer spacer driving the specimen to fracture as soon as the plastic deformation localized. Even if the experiment had been performed using an oil-driven bulge tester this problem would not disappear. The oil is not completely incompressible, and it will store energy, as well.

Obtaining accurate uniaxial data presents difficulties, too. In the case of our conventional uniaxial-tensile samples and the hourglass sample of minimum width, 20 mm, the sheet instability originated on the edge of the sample, where the thickness was 0.6 mm, not in a region of the sheet surface. Thus, we would expect a type and intensity of Marciniak defect different than that controlling all of the other stress states in our FLC measurement. In addition, the conventional tensile sample experiences geometric instabilities. In uniaxial-tension, for the conventional tensile-sample geometry, it is well known that the Considère criterion, predicts plastic-flow localization. When we applied this criterion, we found that the geometric instability occurred at a true strain of 0.21. This value is well below that which would be expected in a sheet-stretching forming operation. Such a low value indicates that, for our material, circle gridding a conventional tensile sample will not generate reliable data for a FLC plot.

Some of the most reliable FLC data we obtained were in the state of plane strain. There was little separation between uniform and localized deformation states, indicating a critical strain where deformation localizes. In this case, the necking instability clearly originated on the sheet surface, in the manner modeled by the Marciniak defect in our simulations. From this standpoint, anchoring our simulations at plane-strain is an obvious choice. Generally, if a sheet fails during forming, it will fail in plane strain. This strain state is also central to the FLC, helping to minimize errors in the VPSC modeling predictions.

As a part of this investigation, we tried to minimize the inputs to the VPSC model. In this spirit, we were able to accomplish the simulations of the unconstrained and free compression experiments, Part I, with only a quantitative texture measurement and fits of hardening laws to uniaxial tensile data. No additional fits were required to predict our steel's Lankford coefficients as a function of angle to the rolling direction. Considering the minimal number of free parameters and data input for these simulations, the agreement between simulation and experiment was excellent. In order to simulate the FLC one more experiment was required, to specify the value of the Marciniak defect. We used an FLC test in plane strain for this purpose. Thus, the entire FLC prediction required only a tensile test, plane-strain FLC measurement and quantitative texture evaluation. Our success with such minimal inputs is perhaps fortuitous and for other materials it is possible that additional inputs will be required.

In summary, we have presented a compilation of material property measurements intended to both calibrate and verify models designed to predict FLC and Lankford behavior in materials used in sheet-forming operations. The measurements intended for input to the simulations include quantitative texture analysis, tensile tests and a plane-strain FLC experiment. To verify the predictions derived from these simulations, we measured channel-die and through-thickness compression constitutive responses and determined a complete FLC curve as well as values of the Lankford coefficient in 15° increments from the rolling to transverse sheet directions.

## Acknowledgements

The authors thank both the Nibbler (Rosario, Santa Fe Province, Argentina) and MEGBA (Granadero Baigorria, Santa Fe Province, Argentina) companies for their collaboration in the preparation of samples and the heat treatment of the dies and punches used to perform these experiments. We also wish to acknowledge the work of Wadi Chiaparoli of IAS and Elena Brandaleze of UTN (San Nicolas, Buenos Aires Province) in applying the circle-grid patterns to the FLC samples. This research is a part of a program funded through a grant from CONICET (National Government of Argentina).

## References

Abedrabbo, N., Pourboghrat, F., Carsley, J., 2006. Forming of aluminum alloys at elevated temperatures – Part 2: numerical modeling and experimental verification. Int. J. Plast. 22, 342–373.

Aghaie-Khafri, M., Mahmudi, R., Pishbin, H., 2002. Role of yield criteria and hardening laws in the prediction of forming limit diagrams. Metall. Mater. Trans. A 33A, 1363–1371.

Aretz, H., 2007. Numerical analysis of diffuse and localized necking in orthotropic sheet metals. Int. J. Plast. 23, 798–840.

Azrin, M., Backofen, W.A., 1970. The deformation and failure of a biaxial stretched sheet. Met. Trans. 1, 2857–2861.

Barlat, F., Brem, J.C., Yoon, J.W., Chung, K., Dick, R.E., Lege, D.J., Pourboghrat, F., Choi, S.-H., Chu, E., 2003. Plane stress yield function for aluminum alloy sheets – part 1: theory. Int. J. Plast. 19, 1297–1319.

Campos, H.B., Butuc, M.C., Grácio, J.J., Rocha, J.E., Duarte, J.M.F., 2006. Theoretical and experimental determination of the forming limit diagram for the AISI 304 stainless steel. J. Mater. Process. Technol. 179, 56–60.

Ganjiani, M., Assempour, A., 2007. An improved analytical approach for determination of forming limit diagrams considering the effects of yield functions. J. Mater. Process. Technol. 182, 598–607.

Ghosh, A.K., Hecker, S.S., 1974. Stretching limits in sheet metals: in-plane versus out-of-plane deformation. Metall. Trans. A 5A, 2161–2164.

Gupta, A.K., Ravi Kumar, D., 2006. Formability of galvanized interstitial-free steel sheets. J. Mater. Process. Technol. 172, 225–237.

Hecker, S.S., 1975. Simple technique for determining FLC. Sheet Met. Ind. 52, 671–675.

Hiroi, T., Nishimura, H., 1997. The influence of surface defects on the forming-limit diagram of sheet metal. J. Mater. Process. Technol. 72, 102–109.

Holmberg, S., Enquist, B., Thilderkvist, P., 2004. Evaluation of sheet formability by tensile tests. J. Mater. Process. Technol. 145, 72–83.

Hutchinson, J.W., Neale, K.W., 1978. Sheet necking II, time-independent behavior. In: Koistinen, D.P., Wang, N.M. (Eds.), Mechanics of Sheet Metal Forming. Plenum Press, New York, London, pp. 127–153.

Janssens, K., Lambert, F., Vanrostenberghe, S., Vermeulen, M., 2001. Statistical evaluation of the uncertainty of experimentally characterised forming limits of sheet steel. J. Mater. Process. Technol. 112, 174–184.

Keeler, S.P., Backhofen, W.A., 1964. Plastic instability and fracture in sheet stretched over rigid punches. ASM Trans. Quart. 56, 25–48.

Kim, K.J., Kim, D., Choi, S.H., Chung, K., Shin, K.S., Barlat, F., Oh, K.H., Youn, J.R., 2003. Formability of AA5182/polypropylene/AA5182 sandwich sheets. J. Mater. Process. Technol. 139, 1–7.

Knockaert, R., Chastel, Y., Massoni, E., 2002. Forming limits predictions using rate-independent polycrystalline plasticity. Int. J. Plast. 18, 231–247.

Kuroda, M., Kuwabara, T., 2002. Shear-band development in polycrystalline metal with strength-differential effect and plastic volume expansion. Proc. R. Soc. Lond. A 458, 2243–2259.

Lebensohn, R.A., Tomé, C.N., 1993. A self-consistent approach for the simulation of plastic deformation and texture development of polycrystals: application to Zr alloys. Acta Metall. Mater. 41, 2611–2624.

Marciniak, Z., Kuczynski, K., 1967. Limit strains in the processes of stretch-forming sheet metal. Int. J. Mech. Sci. 9, 609–620.

McGinty, R.D., McDowell, D.L., 2004. Application of multiscale crystal plasticity models to forming limit diagrams. J. Eng. Mater. Technol. 126, 285–291.

Narayanasamy, R., Sathiya Narayanan, C., 2006. Some aspects on fracture limit diagram developed for different steel sheets. Mater. Sci. Eng. A417, 197–224.

Raghavan, K.S., 1995. A simple technique to generate in-plane forming limit curves and selected applications. Metall. Mater. Trans. A 26A, 2075–2084.

Ravi Kumar, D., 2002. Formability analysis of extra-deep drawing steel. J. Mater. Process. Technol. 130–131, 31–41.

Signorelli, J.W., Bertinetti, M.A., Turner, P.A., 2009. Predictions of forming limit diagrams using a rate-dependent polycrystal self-consistent plasticity model. Int. J. Plast. 25, 1–25.

Wu, P.D., Neale, K.W., Van der Giessen, E., 1997. On crystal plasticity FLD analysis. Proc. R. Soc. Lond. A 453, 1831–1848.

Wu, P.D., Jain, M., Savoie, J., MacEwen, S.R., Tugcu, P., Neale, K.W., 2003. Evaluation of anisotropic yield functions for aluminum sheets. Int. J. Plast. 19, 121–138.

Yoshida, K., Kuwabara, T., Kuroda, M., 2007. Path-dependence of the forming limit stresses in a sheet metal. Int. J. Plast. 23, 361–384.